Numerical Assessment of Electromagnetic Energy and Forces in Non-destructive Measurement Devices

Marilena Stanculescu, Paul Cristian Andrei, Horia Andrei, Sorin Deleanu, and Lavinia Bobaru

Abstract Non-destructive testing in the electromagnetic field is one of the fastest and least expensive testing techniques for pieces subject to degradation. This domain has evolved a lot in recent years, because of the increasing demands received by the scientific community from the industry. Non-destructive testing aims to detect defects (different types of cracks, structural inhomogeneity) in materials (conducting, ferromagnetic) without destroying the tested object. Therefore, the application of such techniques addresses many relevant domains that require high security of installations, domains such as aeronautical, nuclear, medical, or chemical industry. This chapter provides insight into the most commonly used non-destructive measurement devices, but also into the magnetic field analysis in nonlinear media. It presents the magnetization characteristic evaluation for ferromagnetic bodies.

Keywords Non-destructive testing · Numerical methods · Magnetic field · Measurement devices

M. Stanculescu (✉) · P. C. Andrei · L. Bobaru
Department of Electrical Engineering, University Politehnica Bucharest, Bucharest, Romania
e-mail: marilena.stanculescu@upb.ro

P. C. Andrei
e-mail: paul.andrei@upb.ro

L. Bobaru
e-mail: lavinia.bobaru@upb.ro

H. Andrei
Department of Doctoral School, University Valahia, Targoviste, Romania
e-mail: hr_andrei@yahoo.com

S. Deleanu
Northern Alberta Institute of Technology, Edmonton, Canada
e-mail: sorind@nait.ca

N. Mahdavi Tabatabaei and N. Bizon (eds.), *Numerical Methods for Energy Applications*, Power Systems,
https://doi.org/10.1007/978-3-030-62191-9_21

Nomenclature

A. Acronyms

NDT	Non-destructive testing
FEM	Finite Element Method
FEM-BEM	Finite Element Method—Boundary Element Method
SST	Single Sheet Tester
VSM	Vibrating Sample Magnetometer
EMF	Electromotive force
PFPM	Polarization of the Fixed-Point Method

B. Symbols/Parameters

B	Magnetic flux density (induction)
H	Magnetic field strength (intensity)
D	Electric displacement
E	Electric field strength
ε	Absolute permittivity
μ	Absolute permeability
Ψ_{S_Γ}	Electric flux
Φ_{S_Γ}	Magnetic flux
P	Power
X_k	Generalized force
dx_k	Elementary variation
dL_k	Elementary mechanical work
W	Electromagnetic energy
w	Volumetric density of electromagnetic field energy
W_e	Energy of the electric field
W_m	Energy of magnetic field
$w_{h,cycle}$	Volumetric density of the energy transferred by the electromagnetic field to bodies during a full hysteresis cycle, electric and magnetic
w^*	Volume density of electromagnetic field coenergy
w_e^*	Volumetric density of electric coenergy
w_m^*	Volumetric density of magnetic coenergy
p_h	Volumetric density of power transferred by the field
$\overline{S}$	Poynting vector
$\mathbf{J}$	Current density
i	Current
(Σ)	Closed surface
(V_Σ)	Domain bounded by the closed surface (Σ)
(Γ_{el})	Closed contour corresponding to electric hysteresis cycle
$\left(\Gamma_{mg}\right)$	Closed contour corresponding to magnetic hysteresis cycle
$\mathrm{A_{el}}$	Area of electric cycle
$\mathrm{A_{mg}}$	Area of magnetic cycle
$\overline{dA}$	Area element

1 Introduction to Non-destructive Testing

Non-destructive testing(NDT) plays a fundamental part by ensuring the fact that pieces of equipment belonging to a particular structure perform their specific functions for a predetermined amount of time. The specialists in the non-destructive testing field have created and implemented tests to characterize the materials or to detect, localize and measure the flaws (defects) which can case plane crushes, nuclear power plant explosions, train derailment, fires and q whole range of events, less visible, but with very dangerous and with high impact [1].

Because NDT does not, affect in any way the integrity of the product under test, its utilization on a large scale in controlling the quality of the product [2] becomes obvious. Because of its non-destructive nature, the NDT is similar to the medical tests performed on humans or animals. Although, some of the terms used in NDT are synonyms, from the technical point of view by non-destructive evaluation one understands, first of all, the measurement and the description of a defect, the establishment of the its shape and position, the determination, for a material, of the its characteristics, physical, magnetic properties [3–5].

NDT is useful to explore the material integrity of the object under test. Whereas the measurements performed in several areas of science and technology, such as astronomy, radio, electricity (e.g., voltage and current measurement) qualify as non-destructive tests, yet they do not evaluate properties of materials, is specified manners. NDT practically deals with the performance of the equipment under test and answers the question: For how long one can use that piece be safely, and when it needs to be re-tested [6, 7]?

Non-destructive testingin the electromagnetic fieldis one of the fastest and least expensive testing techniques for pieces subject to degradation. This domain has evolved a lot in recent years, because of the increasing demands received by the scientific community from the industry.

Non-destructive testing aims to detect defects (different types of cracks, structural inhomogeneity) in materials (conducting, ferromagnetic) without destroying the tested object. Therefore, the application of such techniques addresses many relevant domains that require high security of installations, domains such as aeronautical, nuclear, medical, or chemical industry.

The researches in non-destructive testing in the electromagnetic field consider important the following two principal directions:

- Flaw (defect) detection
- Flaw shape reconstruction.

Flaw shape reconstruction is an actual domain, drawing huge financial efforts. There are numerous and prestigious international conferences and publications dedicated to this field [1, 8–37].

This chapter starts by giving an introduction in non-destructive testing by highlighting its importance regarding the safety that parts of a structure perform their working functions for a pre-determined period. Non-destructive testing does not

affect the integrity of the body under test, becoming therefore very important for quality control of the product, which is or will be in use. The specialists in this domain have created and implemented methods and devices to characterize the materials or to detect, localize and measure the flaws (defects) with the purpose of preventing events with a high-impact such as plane crushes, nuclear power plant explosions, derailment of trains and other events which are less visible but also dangerous.

The researches in the field of non-destructive testing in the electromagnetic field are oriented into two directions: flaw detection and flaw reconstruction. If the flaw is a crack, then the use of eddy currents testing is the most suitable procedure. For the ferromagnetic pieces, eddy currents testing has significant disadvantage: due to the big permeability, the penetration depth is very small, so only surface defects will be detected. For ferromagnetic body flaws, the best procedure is the use of difference static magnetic field. We have a magnetic field problem in steady-state, but we must deal with the non-linearity of the medium. Because flaw reconstruction implies a huge computation time for the direct problem, one of the main objectives is to obtain procedures for rapid computation of the electromagnetic field in linear/nonlinear media. Many papers in literature recommend the finite element method (FEM) or the hybrid method (Finite Element Method—Boundary Element Method (FEM–BEM)).

The modification of the B-H characteristic, in aged areas, suggests the possibility of elaborating some electromagnetic detection and reconstruction procedures. The computation of the difference static magnetic field seems to be the best procedure. Because the change of the B-H characteristic is very small, it is necessary to obtain a high accuracy computation of the magnetic field in the measurement points.

This chapter falls within the field of non-destructive assessment methods by determining the B-H characteristic of ferromagnetic bodies, by using, for example, a device and a procedure for measuring the first magnetization characteristic.

The main objective of this chapter is the electromagnetic field analysis, together with techniques for determining the corresponding relations. There will be used numerical methods and methods for nonlinearity treatment of the magnetization characteristics, such that the time and the resources allocated for computation to be minimized.

To accomplish the above-proposed objectives, in this chapter, there will be presented the main non-destructive measurement devices, in correlation with related applications. Special attention will be given to those devices used to characterize the magnetic materials widely used in energy generation, distribution and conversion, in telecommunication, aeronautics, etc.

It follows a presentation of the magnetic field analysis methods in nonlinear media. As an example, the study of the magnetization characteristic evaluation for ferromagnetic bodies will be given.

The chapter ends with conclusions and a large number of references in the non-destructive testing and electromagnetic field computation.

2 Non-destructive Measurement Devices

2.1 Description of the Main Devices Utilized for Characterization of the Magnetic Materials

Presently, the utilization of the magnetic materials covers essential domains such as energy distribution and conversion, information transmission and storage, in aeronautics. This fact gives an important reason to demand the measurement of magnetic properties with very high accuracy. Regarding the development of magnetic materials for research and industry use, one of the significant worldwide concern is maintaining the high standard of measurements [38].

At present, many laboratories are using a wide range of characterization devices to determine the magnetic materials properties. The most common devices are Epstein frame, Single Sheet Tester (SST), magneto-optic devices, and Vibrating Sample Magnetometer (VSM).

In [38, 39], the authors analyzed the most extensively used pieces of equipment and methods to determine the characteristics of magnetic materials. There are industrial and laboratory devices presented, accompanied by measurements performed to test their functioning and offer a solution for the complex characterization of soft magnetic material. There are essential aspects regarding the primary devices, and measuring procedures presented in [38–47].

2.2 Epstein Frame

Epstein frame is utilized to determine the electrical steel sheets and strips magnetic properties. The Epstein frame (Fig. 1) consists of four strips placed such that to form a square, with a standard width of 30 mm and length between 280 and 305 mm.

The measurement of electrical steel sheets magnetic properties using the Epstein frame demands the determination of the magnetic flux density (induction) B and the magnetic field strength (intensity) H.

The secondary coil of the frame measures the magnetic induction B.

Whereas the variation is sinusoidal, the induced electromotive force in the secondary coil is proportional to the magnetic induction.

Also, the magnetic computation of H requires measuring the value of the magnetization current (primary), followed by the application of Ampere's Theorem along the mean fiber of the Epstein frame's magnetic circuit [39, 40].

Because of its high reproducibility degree, the method of measuring the magnetic materials properties using the Epstein frame represents a widely accepted standard in the industry [11, 13].

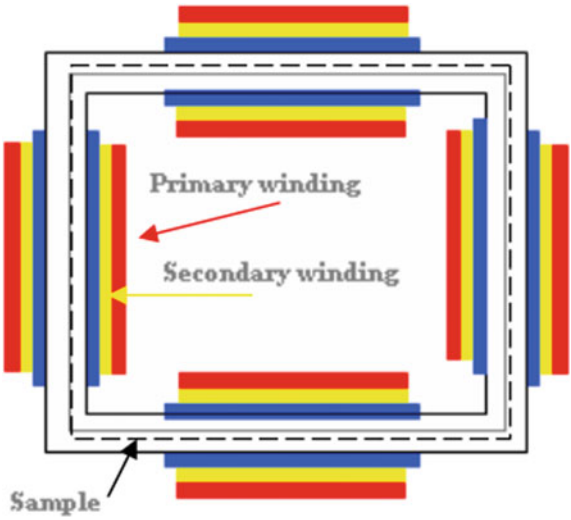

Fig. 1 Epstein frame

2.3 Single Sheet Tester (SST)

Since the Epstein method does not always give the best results, the Single Sheet Tester (SST) which allows the determination of the magnetic field. Several types of SST are used:

– horizontal tester with one frame;

Since the Epstein method does not always give the best results, the Single Sheet Tester (SST) which allows the determination of the magnetic field. There are several SST in use:

– horizontal tester with one frame;
– horizontal tester with two symmetrical frames;
– vertical tester with one frame;
– vertical tester with two symmetrical frames.

A characteristic of the SST method is the fact that there is only one magnetic sheet sample introduced in the space between the two windings: outer primary utilized for magnetization and secondary, which is inner and used to measure the magnetic induction.

For double frames horizontal SST, the frame assembly required the overlapping of metal sheets made from FeSi, with oriented crystals (GO), having a height of 0.1 m [41, 42].

The frame symmetry provokes a systematic error in the measurements because of the eddy currents, which appear in the lamination plane. The eddy currents are the results of the magnetic flux generated by the primary winding, which leaves the measured sample and enters the frame.

For single vertical frame SST, there is a constant error [11, 17–19, 38, 39], called end error when the sample is longer than the frame.

The end error can be eliminated by using symmetrical frames horizontal or vertical and by placing the sample between the two identical frames. If the target is the correct measurement of the tangential component of the magnetic field, which varies with distance, x at the sheet's surface, then two field coils are used. The measurement of the laminated sheets magnetic properties and the determination of the effective value of H, eliminating the approximation made regarding the length of the magnetic circuit, is done using the field coil method.

2.4 Magneto-optic Investigation Methods of the Magnetic Domain Structures

Due to this fact, the domain whose magnetizations are oriented differently, determine the different rotation of the reflected or transmitted light polarization plane [39, 43–45].

The measuring method based on the Kerr effect consists of directing a rectilinear polarized light fascicle using a Nicol prism. The reflected fascicle is going through an analyzer, which is, in fact, another Nicol prism. The transmission plane is practically in a right angle with the polarizer, ensuring, therefore, the extinction for a given magnetic state. The apparition of alternating bands, dark or bright when the prism rotates until it reaches an adequate position, underlines the existence of the domains. The contrast is optimum when the rectilinear incident vibration is almost parallel (t) or normal (n) to the plane of incidence, and the experience fully confirmed the theory [46].

The Kerr method requires special treatment of the sample surface but it applies to a vast range of temperatures and excitation field values.

2.5 Vibrating Sample Magnetometer (VSM)

Vibrating Sample Magnetometer (VSM) consists of a magnetized sample. VSM performs an oscillation movement inside a system of coils, such that inside, it induces an electromotive force (EMF) proportional to the sample's magnetic moment. If there is a magnetic dipole Q_{1z} which vibrates along the z-axis with amplitude δz, and the angular frequency of the vibration is ω, the dipole's position function of time is $z = \delta z(\cos\omega t)$. Such a scenario may be equivalent to the situation of a stationary quadrupole.

In his case, a system of coils system, sensitive to the quadrupole's vibrations can produce, a field with homogenous gradient $\partial H_z/\partial z$ with the assumption that an electric current is flowing through its windings. Inside the domain of homogeneity

for the gradient $\partial H_z/\partial z$, the sensitivity of coils with respect to the dipole's movement does not depend on the position of the volume of the dipole [41, 47].

The pair of coils, placed inside of the air-cored solenoid, may generate a magnetic field. The dipolar moment is equal to zero, being independent on the variations of the applied homogenous field. When the second-order derivative of the outer magnetic field has a significant value, then the detection coils can measure an induced EMF, leading to measurement errors. This fact recommends the introduction of an extra pair of coils able to cancel the induced EMF.

The connection of the outer coils is "series-opposition" having a big quadripolar moment to cancel the quadripolar moment from the central coils. A voltage divider was able to balance the system.

3 Numerical Assessment of Electromagnetic Energy and Forces

3.1 Electromagnetic Field Energy Theorem

The presentation of this theorem starts with two remarks [48]:

1. The first one refers to the importance of this theorem, importance that consists in the fact that it underlines *the electromagnetic fieldcapacity to accumulate and transfer energy.*
2. The second one refers to the hypothesis used to prove this theorem, more precisely: the bodies are at rest, and the media are linear, isotropic, and without permanent electric polarization and permanent magnetization. At the end of the proof, we have made observations regarding the influence of the adoption of these hypotheses upon the generality degree of the theorem.

Let us consider a closed surface (Σ) that bounds a domain (V_Σ) in which coexist the energetic interaction between the bodies (i.e., forms of matter, material substance) and the electromagnetic field. For the assumptions made above, the local forms of electromagnetic induction law, respectively magnetic circuit law for domains with continuity, show that in any point from domain (V_Σ) and for any instance of time, t there are the following relations in place:

$$\begin{aligned} curl\,\overline{E} &= -\frac{\partial \overline{B}}{\partial t} \\ curl\,\overline{H} &= \overline{J} + \frac{\partial \overline{D}}{\partial t}\,. \end{aligned} \tag{1}$$

Combining the two relations (1) results:

$$-\left(\overline{E}\cdot\frac{\partial\overline{D}}{\partial t}+\overline{H}\cdot\frac{\partial\overline{B}}{\partial t}\right)=\overline{E}\cdot\overline{J}+div\left(\overline{E}\times\overline{H}\right). \tag{2}$$

For linear media, isotropic and without permanent electric polarization or permanent magnetization, of absolute permittivity ε and absolute permeability μ, the constitutive laws have the forms $\overline{D}=\varepsilon\cdot\overline{E}$ and, respectively, $\overline{B}=\mu\cdot\overline{H}$, whereas the processing of the terms $\overline{E}\cdot\frac{\partial\overline{D}}{\partial t}$ and $\overline{H}\cdot\frac{\partial\overline{B}}{\partial t}$ gives:

$$-\frac{\partial}{\partial t}\left(\frac{\overline{D}\cdot\overline{E}}{2}+\frac{\overline{B}\cdot\overline{H}}{2}\right)=\overline{E}\cdot\overline{J}+div\left(\overline{E}\times\overline{H}\right). \tag{3}$$

Furthermore, to obtain global information concerning the electromagnetic phenomena from the domain (V_Σ), one can proceed as follows:

Computation of the space integral results into:

$$-\frac{\partial}{\partial t}\int\limits_{(V_\Sigma)}\left(\frac{\overline{D}\cdot\overline{E}}{2}+\frac{\overline{B}\cdot\overline{H}}{2}\right)\cdot dv=P+\int\limits_{(\Sigma)}\left(\overline{E}\times\overline{H}\right)\cdot\overline{dA}_{ext}. \tag{4}$$

Analyzing the above relation from a dimensional perspective and remarking that only one integral term contains the quantities defining the electromagnetic field, one can conclude that the surface integral

$$P_\Sigma=\int\limits_{(\Sigma)}\left(\overline{E}\times\overline{H}\right)\cdot\overline{dA}_{ext} \tag{5}$$

has the significance of a power, i.e., *the power transferred by that the electromagnetic fieldthrough the boundary* (Σ), while the volume integral

$$W=\int\limits_{(V_\Sigma)}\left(\frac{\overline{D}\cdot\overline{E}}{2}+\frac{\overline{B}\cdot\overline{H}}{2}\right)\cdot dv \tag{6}$$

has the significance of an energy, i.e., *the electromagnetic fieldenergy from the domain* (V_Σ).

The identity

$$-\frac{\partial W}{\partial t}=P+P_\Sigma \tag{7}$$

defines an equation referring to the power balance. It represents the mathematical expression of the electromagnetic energy theorem, which states: *The time variation*

of the electromagnetic field energy W from domain (V_Σ) *is equal to the sum between the power P transferred from the field to the bodies within the domain* (V_Σ) *during the electric conduction process, and the power* P_Σ *transferred by the field to the domain's exterior through the boundary* (Σ).

In the power balance equation, the quantity W is positively defined, whereas the quantities P and P_Σ can be either positive or negative depending on the problem under scrutiny. For the computation of term P_Σ, the vectorized area element $\overline{dA}$ points towards the exterior of the closed surface (Σ).

Meanwhile, the signs in front of the scalars P, P_Σ and $\frac{\partial W}{\partial t}$ show the real directions of the energy transfer, as follows:

(1) $P > 0$: the electromagnetic field transfers power from the domain (V_Σ) to the bodies from the domain (V_Σ) during the electric conduction process
(2) $P < 0$: the bodies from domain (V_Σ) transfer power to the electromagnetic field during the electric conduction process
(3) $P_\Sigma > 0$: the electromagnetic field transfers power through the boundary (Σ)
(4) $P_\Sigma < 0$: the electromagnetic field receives power through the boundary (Σ)
(5) $\left(-\frac{\partial W}{\partial t}\right) > 0$: the energy of the electromagnetic field from the domain (V_Σ) decreases in time
(6) $\left(-\frac{\partial W}{\partial t}\right) < 0$: then the energy of the electromagnetic field from the domain (V_Σ) increases in time.

Figure 2 illustrates the case: $P > 0$, $P_\Sigma > 0$.

According to the energy localization principle, the quantity:

$$w = \frac{\overline{D} \cdot \overline{E}}{2} + \frac{\overline{B} \cdot \overline{H}}{2} \tag{8}$$

represents the volumetric density of the electromagnetic field energy from the domain (V_Σ) and it has two components:

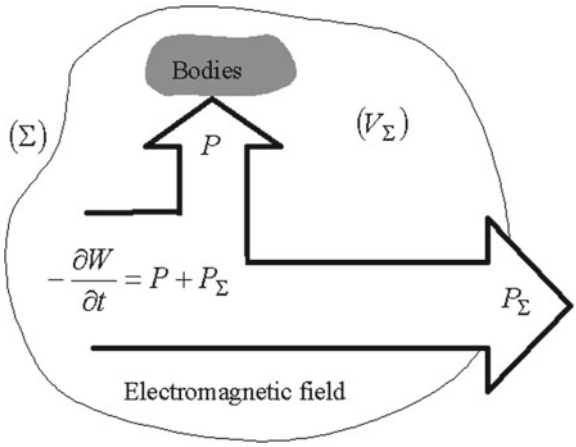

Fig. 2 Qualitative illustration of the electromagnetic field

(a) The volumetric density of electric energy:

$$w_e = \frac{\overline{D} \cdot \overline{E}}{2} \tag{9}$$

(b) The volumetric density of the magnetic energy

$$w_m = \frac{\overline{B} \cdot \overline{H}}{2}\,. \tag{10}$$

Consequently, the next identity results from a volume integration covering the domain (V_Σ):

$$W = \int\limits_{(V_\Sigma)} \left(\frac{\overline{D} \cdot \overline{E}}{2} + \frac{\overline{B} \cdot \overline{H}}{2} \right) \cdot dv = \int\limits_{(V_\Sigma)} w_e \cdot dv + \int\limits_{(V_\Sigma)} w_m \cdot dv = W_e + W_m\,, \tag{11}$$

Relation (11) demonstrates that the energy W of the electromagnetic field is the sum between the energy W_e of the electric field (12) and the and energy W_m of the magnetic field (13).

$$W_e = \int\limits_{(V_\Sigma)} w_e \cdot dv \tag{12}$$

$$W_m = \int\limits_{(V_\Sigma)} w_m \cdot dv. \tag{13}$$

The quantity

$$\overline{S} = \left(\overline{E} \times \overline{H}\right) \tag{14}$$

is called Poynting vector and has as the significance of the electromagnetic power flux density through the boundary (Σ), respectively the "flow" speed of electromagnetic energy through this surface:

$$P_\Sigma = \int\limits_{(\Sigma)} \overline{S} \cdot \overline{dA}_{ext} = \int\limits_{(\Sigma)} \left(\overline{S} \cdot \overline{n}\right) \cdot dA\,. \tag{15}$$

The vector $\overline{S}$ has the form

$$\overline{S}^{'} = \left(\overline{E} \times \overline{H}\right) + \overline{S}^{''} \tag{16}$$

with $\overline{S}''$ a zero-divergence vector.

3.2 *Electromagnetic Field Energy and Coenergy for Nonlinear Media*

Let us consider again a closed surface (Σ) that bounds a domain (V_Σ) in which coexist bodies and electromagnetic field in energetic interaction. From the set of adopted hypotheses required to prove the electromagnetic energy theorem, one must eliminate the assumption referring to the linear character of media.

However, the hysteresis of media does not play any role this time (i.e., media without hysteresis).

As shown previously, the immobility of the bodies and the inexistence of the hysteresis indicates that $P_m = P_h = 0$ and subsequently, the first principle of thermodynamics has the form:

$$-\frac{\partial W}{\partial t} = P + P_\Sigma \,. \tag{17}$$

The relationship (18)

$$-\left(\overline{E}\cdot\frac{\partial \overline{D}}{\partial t} + \overline{H}\cdot\frac{\partial \overline{B}}{\partial t}\right) = \overline{E}\cdot\overline{J} + div\left(\overline{E}\times\overline{H}\right) \tag{18}$$

was proved in the above paragraph using the local forms of the electromagnetic induction law and magnetic circuit law and, consequently, stays valid for any type of media, including the nonlinear ones.

From (19)

$$-dW = (P + P_\Sigma)\cdot dt \tag{19}$$

and (20)

$$-\int\limits_{(V_\Sigma)} \left(\overline{E}\cdot d\overline{D} + \overline{H}\cdot d\overline{B}\right)\cdot dv = (P + P_\Sigma)\cdot dt \tag{20}$$

results the expression of variation dW of electromagnetic field energy during that transformation (21):

$$dW = \int\limits_{(V_\Sigma)} \left(\overline{E}\cdot d\overline{D} + \overline{H}\cdot d\overline{B}\right)\cdot dv \,. \tag{21}$$

Using again the principle of energy localization (22)

$$dW = \int\limits_{(V_\Sigma)} dw \cdot dv\,, \tag{22}$$

results the variation dw of the volumetric density of electromagnetic field energy as:

$$dw = \overline{E} \cdot d\overline{D} + \overline{H} \cdot d\overline{B} \tag{23}$$

The two components of dw are:

– variation dw_e of the volumetric density of electric energy

$$dw_e = \overline{E} \cdot d\overline{D} \tag{24}$$

– variation dw_m of the volume density of magnetic energy

$$dw_m = \overline{H} \cdot d\overline{B} \tag{25}$$

If the media does not have permanent electric polarization, nor permanent magnetization, then the volumetric densities of electric energyw_e, respectively of the magnetic energy w_m corresponding to an arbitrary state characterized by the pair values $\left(\overline{E}, \overline{D}\right)$ respectively, $\left(\overline{H}, \overline{B}\right)$ result from integrations (26) and (27) while the reference state assumes all of the electromagnetic field state quantities equal to zero:

$$w_e = \int\limits_0^{\overline{D}} \overline{E} \cdot \overline{dD} = \int\limits_0^{D} E \cdot dD \tag{26}$$

respectively:

$$w_m = \int\limits_0^{\overline{B}} \overline{H} \cdot \overline{dB} = \int\limits_0^{B} H \cdot dB \tag{27}$$

The volumetric density w of electromagnetic field energy is:

$$w = w_e + w_m\,. \tag{28}$$

The volumetric density of electric coenergy is:

$$w_e^* = \int_0^{\overline{D}} \overline{E} \cdot \overline{dD} = \int_0^D E \cdot dD \tag{29}$$

with the volume density of magnetic coenergy:

$$w_m^* = \int_0^{\overline{B}} \overline{H} \cdot \overline{dB} = \int_0^B H \cdot dB \tag{30}$$

and the volume density w^* of electromagnetic field coenergy is

$$w^* = w_e^* + w_m^* . \tag{31}$$

Figure 3 contains two nonlinear dependencies, one in terms of the electric field (see Fig. 3a) and one in terms of the magnetic field (see Fig. 3b) are qualitatively depicted. The geometric interpretation comes immediately:

- The volumetric density of electric energy w_e, corresponding to electric field state, and characterized by the pair of values (E, D), is represented by the horizontally hatched area bordered by the nonlinear curve $D = D(E)$, OD axis and the horizontal line $D =$ constant,
- The volumetric density of electric coenergyw_e^*, corresponding to electric field state characterized by the pair of values (E, D), is represented by the vertically hatched area included between the nonlinear curve that gives the dependence $D = D(E)$, OE axis and the vertical line $E =$ constant.
- The volumetric density w_m of the magnetic energy, corresponding to magnetic field state characterized by the pair of values (H, B), is represented by the horizontally hatched area bounded between the nonlinear curve that gives the dependence $B = B(H)$, OB axis and the horizontal line $B =$ constant,

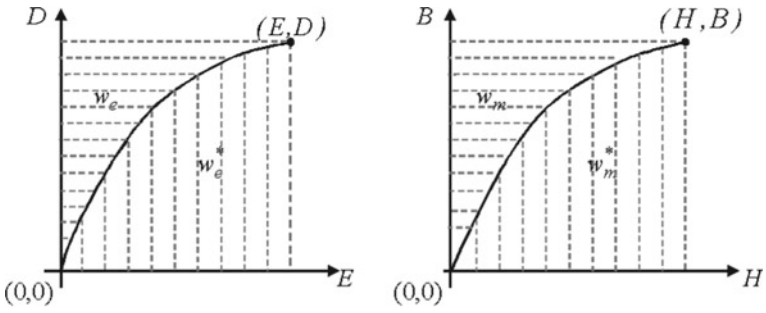

Fig. 3 Generic (qualitative) nonlinear dependencies $D = D(E)$ and $B = B(H)$

– The volumetric density w_m^* of magnetic coenergy, corresponding to magnetic field state characterized by the pair of values (H, B), is represented by the vertically hatched area bounded between the nonlinear curve that gives the dependence $B = B(H)$, OH axis and the vertical line $H = \text{constant}$.

These interpretations prove that:

$$w_e + w_e^* = D \cdot E = \overline{D} \cdot \overline{E} \tag{32}$$

$$w_m + w_m^* = B \cdot H = \overline{B} \cdot \overline{H}, \tag{33}$$

Relations (32) and (33) in the particular case of linear media become:

$$w_e = w_e^* = \frac{\overline{D} \cdot \overline{E}}{2} \tag{34}$$

$$w_m = w_m^* = \frac{\overline{B} \cdot \overline{H}}{2}\,. \tag{35}$$

In this, way we found again the expressions obtained for volume densities of electric energy and, respectively, magnetic energy, this time for linear media.

3.3 Warburg Theorem

The purpose of this theorem is to evaluate a specific experimental finding in terms of quantity. According to the specific experiments, one found that in nonlinear media with hysteresis, the electromagnetic field transfers power to the bodies during the hysteresis cycle. Let us consider again a closed surface (Σ) that bounds a domain (V_Σ) in which coexist bodies (i.e., material) and electromagnetic field in energetic interaction. The end of Sect. 1 shown that the electromagnetic field energy variation (V_Σ) obeys the first principle of thermodynamics, mathematically reflected by the relation:

$$-\frac{\partial W}{\partial t} = P + P_m + P_h + P_\Sigma\,, \tag{36}$$

For immobile bodies $(P_m = 0)$ has the particular form:

$$-\frac{\partial W}{\partial t} = P + P_h + P_\Sigma\,. \tag{37}$$

In this power balance equation, P_h represents the power transferred by the electromagnetic field to the bodies from the domain (V_Σ) through hysteresis. However, the expression of the electromagnetic field energy W is unknown.

The relation

$$-\int\limits_{(V_\Sigma)} \left(\overline{E} \cdot \frac{\partial \overline{D}}{\partial t} + \overline{H} \cdot \frac{\partial \overline{B}}{\partial t} \right) \cdot dv = P + P_\Sigma \tag{38}$$

proven in Sect. 1 using the local forms of electromagnetic induction law and magnetic circuit law. Consequently, it is also valid for media with hysteresis.

Carrying out an elementary transformation results:

$$-dW = (P + P_\Sigma) \cdot dt + P_h \cdot dt \tag{39}$$

and, respectively,

$$-\int\limits_{(V_\Sigma)} \left(\overline{E} \cdot d\overline{D} + \overline{H} \cdot d\overline{B} \right) \cdot dv = (P + P_\Sigma) \cdot dt \tag{40}$$

whereas subtracting member by member:

$$-dW + \int\limits_{(V_\Sigma)} \left(\overline{E} \cdot d\overline{D} + \overline{H} \cdot d\overline{B} \right) \cdot dv = P_h \cdot dt \tag{41}$$

From the principle of energy localization and, respectively, of the power, the variation of electromagnetic field energy volumetric density dw in the domain (V_Σ):

$$dW = \int\limits_{(V_\Sigma)} dw \cdot dv \tag{42}$$

The volumetric density p_h of power transferred by the field to the bodies from the domain (V_Σ) by hysteresis:

$$P_h = \int\limits_{(V_\Sigma)} p_h \cdot dv\,. \tag{43}$$

Then Eq. (41) becomes, assuming the immobile bodies:

$$
\begin{aligned}
&-\int\limits_{(V_\Sigma)} dw \cdot dv + \int\limits_{(V_\Sigma)} \left(\overline{E} \cdot d\overline{D} + \overline{H} \cdot d\overline{B}\right) \cdot dv = \\
&= \left(\int\limits_{(V_\Sigma)} p_h \cdot dv\right) \cdot dt = \int\limits_{V_\Sigma} (p_h \cdot dt) \cdot dv
\end{aligned}
\tag{44}
$$

The equality (41) is true whichever the domain (V_Σ) is, such that the integral equality implies the equality of the integrands:

$$
-dw + \left(\overline{E} \cdot d\overline{D} + \overline{H} \cdot d\overline{B}\right) = p_h \cdot dt \tag{45}
$$

To avoid the complication of finding the instantaneous transfer of power in the hysteresis process, we consider a very frequently case met in practice, namely the case of the electromagnetic fields with periodic time variations (called alternating fields). Let T be the period necessary to traverse an electric hysteresis cycle $\overline{D} = \overline{D}\left(\overline{E}\right)$ and, respectively, a magnetic one, $\overline{B} = \overline{B}\left(\overline{H}\right)$. Integrating with respect to the time variable, one can obtain:

$$
-\int\limits_0^T dw + \int\limits_0^T \left(\overline{E} \cdot \overline{dD} + \overline{H} \cdot \overline{dB}\right) = \int\limits_0^T p_h \cdot dt, \tag{46}
$$

in which the integral

$$
\int\limits_0^T p_h \cdot dt = w_{h,cycle} \tag{47}
$$

represents the volumetric density $w_{h,cycle}$ of the energy transferred by the electromagnetic field to bodies during a full hysteresis cycle, electric and magnetic. Because both, the electromagnetic energy W and the volumetric energy density w (whose expression is unknown) are state functions, it results that:

$$
\int\limits_0^T dw = w(T) - w(0) = 0\,. \tag{48}
$$

Moreover,

$$
\int\limits_0^T \left(\overline{E} \cdot \overline{dD} + \overline{H} \cdot \overline{dB}\right) = \int\limits_0^T (E \cdot dD + H \cdot dB) \tag{49}
$$

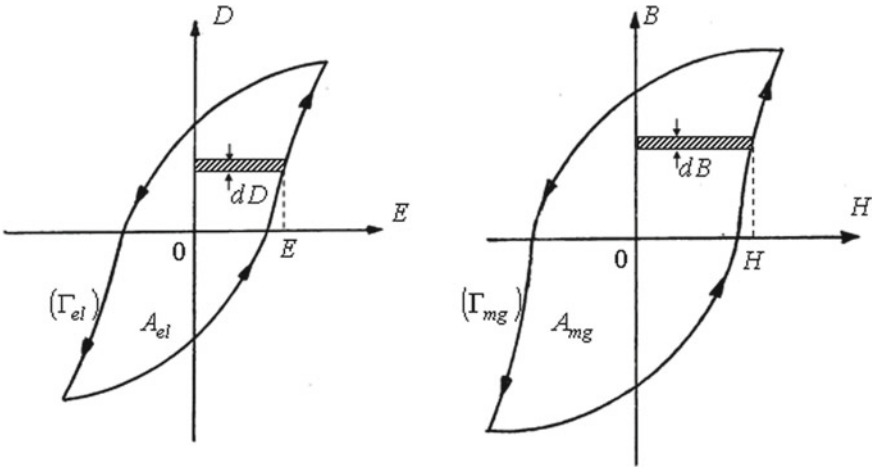

Fig. 4 Hysteresis cycles

the time integration can be interpreted as a space integration for the closed contours (Γ_{el}) and (Γ_{mg}) corresponding to the two hysteresis cycles electric and, respectively, magnetic one (see Fig. 4).

With these assumptions, the volumetric density of the electromagnetic energy for a hysteresis cycle is:

$$w_{h,cycle} = \int_0^T E \cdot dD + \int_0^T H \cdot dB = \int_{(\Gamma_{el})} E \cdot dD + \int_{(\Gamma_{mg})} H \cdot dB = w_{h,el} + w_{h,mg}\,. \tag{50}$$

Relation (50) emphasizes the Warburg theorem: *The two components of the volumetric energy density irreversibly transferred by the electromagnetic fieldto bodies during the two-hysteresiscycles are*:

$$w_{h,el} = \int_{(\Gamma_e)} E \cdot dD = \mathrm{A}_{el} \tag{51}$$

$$w_{h,mg} = \int_{(\Gamma_m)} H \cdot dB = \mathrm{A}_{mg} \tag{52}$$

The terms of relations (51), (52) and have the significations of the areas $\mathrm{A_{el}}$ and $\mathrm{A_{mg}}$ of the cycles. This energy transfer leads to the heating of heating ferroelectric and ferromagnetic bodies by transforming the electromagnetic energy in caloric energy.

3.4 The Generalized Forces Theorem in the Electromagnetic Field

The bodies placed inside the electromagnetic field are subjects to ponderomotive actions: forces, torques, superficial tensions, pressures. This fact inspired the scientists to introduce and utilize the concepts of *generalized coordinate* and *generalized force.* The body exposure to ponderomotive actions can results in the modification of its state due to translations, rotations, or deformations caused by the mechanical work involved. Let us consider again a closed surface (Σ) that bounds a domain (V_Σ) in which coexist bodies (i.e., material) and electromagnetic field in energetic interaction. Moreover, the term: system of bodies with *n degrees of freedom* designates a system completely described by a number of *n scalar independent variables.* The variables are defined as *generalized coordinates* and denoted by $x_1,\ x_2, \ldots, x_n$. If one of the bodies from the system modifies its position, for example, one of its coordinates, x_k may encounter one elementary variation dx_k. This fact signifies an elementary mechanical work dL_k.

The elementary variations dL_k and dx_k are linearly linked (53)

$$dL_k = X_k \cdot dx_k \tag{53}$$

by the proportionality coefficient X_k, called the *generalized force*. It becomes a force (in the current acceptance of the notion) whereas x_k is a length, a torque when x_k is an angle, a superficial tension when x_k is an area, a pressure when x_k is a volume. Furthermore (54) expressed the energy variation in terms of power:

$$-\frac{\partial W}{\partial t} = P + P_m + P_\Sigma \tag{54}$$

and

$$-\int\limits_{(V_\Sigma)} \left(\overline{E} \cdot \frac{\partial \overline{D}}{\partial t} + \overline{H} \cdot \frac{\partial \overline{B}}{\partial t} \right) \cdot dv = P + P_\Sigma \,. \tag{55}$$

Subtracting member by member the relation (54) and (55) one obtains:

$$-\frac{\partial W}{\partial t} + \int\limits_{(V_\Sigma)} \left(\overline{E} \cdot \frac{\partial \overline{D}}{\partial t} + \overline{H} \cdot \frac{\partial \overline{B}}{\partial t} \right) \cdot dv = P_m \,. \tag{56}$$

Theory proven in the past that the elementary mechanical work

$$dL_k = P_m \cdot dt \tag{57}$$

depends on the elementary performed transformation performed, while the generalized forces do not depend on it. Therefore, one can choose, the elementary transformation meant to simplify most of the computations, without diminishing the generality of the conclusions. This elementary transformations refer to the electric fluxes Ψ_{S_Γ} and magnetic fluxes Φ_{S_Γ}, which are time-invariant, through any surface S_Γ. The cancellation of the time derivatives of these fluxes leads to:

$$\frac{\partial \Psi_{S_\Gamma}}{\partial t} = \frac{\partial}{\partial t} \int\limits_{(S_\Gamma)} \overline{D} \cdot \overline{dA} = \int\limits_{(S_\Gamma)} \frac{\partial \overline{D}}{\partial t} \cdot \overline{dA} = 0 \tag{58}$$

and, respectively,

$$\frac{\partial \Phi_{S_\Gamma}}{\partial t} = \frac{\partial}{\partial t} \int\limits_{(S_\Gamma)} \overline{B} \cdot \overline{dA} = \int\limits_{(S_\Gamma)} \frac{\partial \overline{B}}{\partial t} \cdot \overline{dA} = 0\,. \tag{59}$$

Consequently, using the previous equations, results:

$$-\frac{\partial W}{\partial t} = P_m\,, \tag{60}$$

conditions in which, for an elementary transformation, the power balance equation:

$$-dW = P_m \cdot dt = dL_k = X_k \cdot dx_k \tag{61}$$

demonstrates that the elementary mechanical work dL_k is realized exclusively on the decrease of the electromagnetic field energy.

The relation:

$$X_k = -\left(\frac{\partial W}{\partial x_k}\right)\Bigg|_{\Psi,\Phi=ct} \tag{62}$$

represents the mathematical form of the generalized forces theorem in electromagnetic field. This theorem has the following statement: "*The generalized force $X_k$exerted along the generalized coordinate $x_k$is equal to the negative of the partial derivative of the electromagnetic field energy W, function of the generalized coordinate x_k, in conditions of time-invariant electric and magnetic fluxes through any surface.*"

As

$$W = W_e + W_m \tag{63}$$

it results that

$$X_k = -\left(\frac{\partial W}{\partial x_k}\right)\Bigg|_{\Psi,\Phi=ct} = -\left(\frac{\partial W_e}{\partial x_k}\right)\Bigg|_{\Psi=ct} - \left(\frac{\partial W_m}{\partial x_k}\right)\Bigg|_{\Phi=ct}, \tag{64}$$

followed by the particular relations defining the generalized forces theorem in the electric field:

$$X_k = -\left(\frac{\partial W_e}{\partial x_k}\right)\Bigg|_{\Psi=ct} \tag{65}$$

respectively the generalized forces theorem in the magnetic field:

$$X_k = -\left(\frac{\partial W_m}{\partial x_k}\right)\Bigg|_{\Phi=ct} \tag{66}$$

There are few observations valid:

- X_k is a scalar component (affected by sign) of the vector component $\overline{X}_k$ representing the generalized force $\overline{X}$ with respect to the direction of the generalized coordinate x_k
- The sign of the scalar X_k gives the information regarding the direction of the vector component $\overline{X}_k$ from generalized force $\overline{X}$: if $X_k > 0$, then the component $\overline{X}_k$ is oriented in the increasing direction of the generalized coordinate x_k, and if $X_k < 0$, then the component $\overline{X}_k$ is oriented in the decreasing direction of the generalized coordinate x_k
- To compute the generalized force X_k, there is necessary to determine the system degrees of freedom (i.e., their number), to express the electromagnetic field energy W as a function of fluxes and the generalized coordinate x_k and then perform a derivation of the energy expression with respect to x_k, assuming as the electric and the magnetic fluxes are time-invariant.

4 Case of Study

Nowadays, the existing devices and procedures, for determining the ferromagnetic materials' **B-H** relationship, use samples from the studied material. The geometry is imposed by the installation [38, 39]. The excitation current is a time variable. For instance, the Epstein frame measure **B-H** relationships for sheets of precise dimensions, which constitute the 4 branches of the magnetic circuit. The metal sheets interleaving at the frame's corners reduce the reluctance of the air gap between the branches.

Along the magnetic circuit, it is assumed that the magnetic field strength and the magnetic flux density are constant and as a consequence, the value of the current

which power the excitation coils is proportional **H**, and **B** is proportional to the voltage's time integral across the coil which measures the time-varying magnetic flux.

Single Sheet Tester (SST) is a device where the sample consists of a single sheet, which makes the yokes reluctance almost negligible. The magnetic field strength is achieved by measuring the excitation current. In this case, a Rogowski coil is utilized along with the sheet. In this way, the magnetic voltage drops from the yokes are canceled. The magnetic field must be a time-variable.

The devices presented above have some drawbacks, among which we can list:

- they need individual geometry samples (with dimensions which must be well-defined);
- the magnetic field is non-uniform, and the flux leakage is not null;
- the excitation current is time variable to produce a voltage at the terminals of the coil used for measurement;
- a higher voltage value at the terminals of the measuring coil involves a faster time change of the magnetic field, which can lead to the occurrence of eddy currents, thus inducing measurement errors.

One proposes an innovative measuring device [38] for assessing the **B-H** relationship of ferromagnetic materials, using a procedure accurate enough to obtain efficient results. The proposed device has two constructive shapes: one shape for samples, where materials of precise dimensions and geometric shapes are used, respectively, an in-situ shape, which can be used to assess a material of any dimensions or geometric shape.

The proposed device consists of a magnetic circuit (1, 2, 3, 4) like in Figs. 5 or 6, where one of the exterior branches contains the piece/sample (4) whose **B-H** relationship one wants to assess. The materials of the other branches of the magnetic circuit (1, 2, 3) have known **B-H** relationships, with an excellent static relative magnetic permeability. In the center, there is a median yoke (2, 3) interrupted by a small air gap. In the magnetic circuit windows, are placed the coils (5, 6), and excited by the currents i_1 and i_2. One energizes coil 2 with the current i_2, whereas its value is increasing in steps. For each value of i_2, one searches the value of current i_1 from coil 1 for which the magnetic flux through the median yoke (2, 3) is null (=0).

In the median yoke air gap, along the air gap, there are several Hall probes (7) placed in point equally distributed, such that the sum of the transversal components of the magnetic flux densities measured by these probes to allow us to decide whether the magnetic flux in the median yoke is zero (=0).

In Table 1 are described the components from which the measuring device is built.

Following the measurements presented above, one obtains a string of pairs ($i_1^{(k)}$, $i_2^{(k)}$), representing the currents from coils 1 and 2, for which the magnetic flux in the median yoke is zero. The procedure involved in the calculation of the **B-H** relationship for the piece (sample) is the following:

(1) For the first pair ($i_1^{(1)}, i_2^{(1)}$) one computes the magnetic field (**B, H**). The following equations are verified:

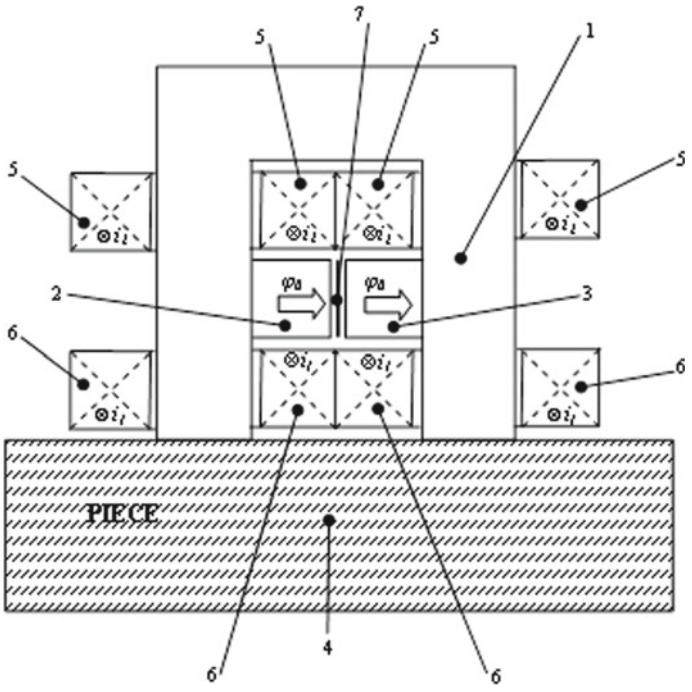

Fig. 5 In-situ measuring device

$$\nabla \times \mathbf{H} = \mathbf{J}, \tag{67}$$

$$\nabla \cdot \mathbf{B} = 0, \tag{68}$$

$$H = \frac{B}{\mu_0}, \text{ in air}, \tag{69}$$

$$\mathbf{H} = F(\mathbf{B}), \text{ in the magnetic material of the device}, \tag{70}$$

where $\mathbf{J}$ is the current density imposed by the currents $i_1^{(1)}$, $i_2^{(1)}$ circulating through the two coils. For the studied sample, one assumes that the B-H relationship starts linearly from the origin, with a slope μ(i.e., considering the sample material isotropic and homogenous):

$$H = \frac{B}{\mu} \tag{71}$$

(2) Then one determines the flux ϕ_0 and searches the value $\mu^{(1)}$ for which $\phi_0 = 0$, then calculates the maximum value $B^{(1)}$ from the sample. For $B \in [0, B^{(1)}]$, the

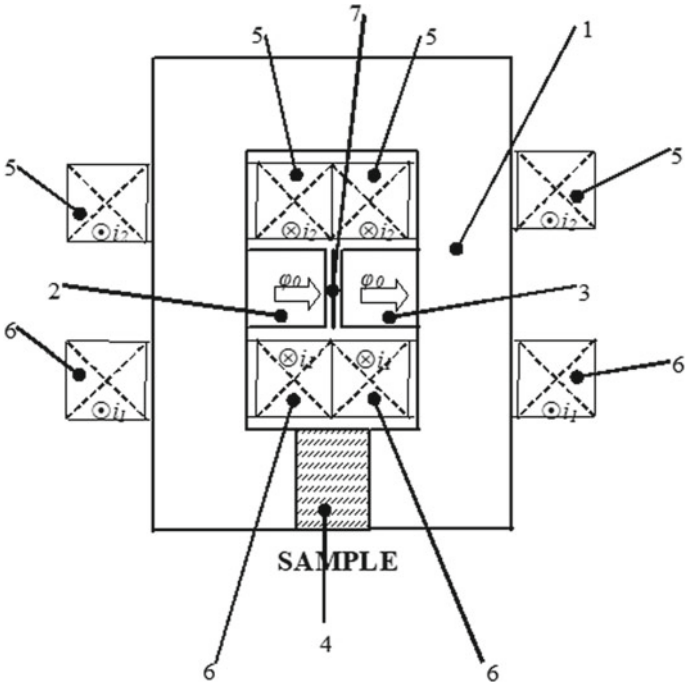

Fig. 6 Sample measuring device

Table 1 Components of the measuring device

Crt. no	Constitutive element
1	Device magnetic circuit—lateral and transversal yokes
2	Left median yoke
3	Right median yoke
4	Piece/sample
5	Coil_2
6	Coil_1
7	Hall probes

B-H relationship is described by the line of slope $\mu^{(1)}$:

$$H = \frac{B}{\mu^{(1)}}. \tag{72}$$

To determine the value of $\mu^{(1)}$, the secant method can be used.

(3) Next, for the pair $(i_1^{(2)}, i_2^{(2)})$ one determines the magnetic field which verifies the Eqs. (67)–(70). For the studied sample, one searches the linear extension of

the *B-H* relationship over the value $B^{(1)}$ and then searches for the slope $\mu^{(2)}$ for which $\phi_0 = 0$. This slope is valid for $B \in [B^{(1)}, B^{(2)}]$, where $B^{(2)}$ represents the newly sample's maximum value of the magnetic flux density. The extension of the B-H relationship becomes:

$$H = \begin{cases} \frac{B}{\mu^{(1)}}, & pt.\ B \in [0, B^{(1)}] \\ H - H^{(1)} = \dfrac{B - B^{(1)}}{\mu^{(2)}}, & pt.\ B \in [B^{(1)}, B^{(2)}] \\ \ldots & \\ H - H^{(n)} = \dfrac{B - B^{(n)}}{\mu^{(n+1)}}, & pt.\ B \in [B^{(n)}, B^{(n+1)}] \end{cases} \tag{73}$$

(4) The application of the method/algorithm continues in the same way, eventually obtaining the piecewise linear *B-H* relationship of the sample. The piecewise linear approximation is as smoother as we choose a smaller step Δi_2.

This device has the following advantages:

- One has to measure only two currents of the coils under the conditions of zero value of the magnetic flux through the median yoke ($\phi_0 = 0$).
- The measurement of the magnetic flux through the median yoke is not necessary; one just needs to ensure that it has a zero value (like Wheatstone bridge).
- When computing the magnetic field, the material and the form of the median yoke can be randomly adopted.
- The measuring procedure is not conditioned by the time variation of the currents through the coils.

The algorithm used to reconstruct the B-H relationship is based on a FEM program coupled with the *polarization of the fixed-point method* (PFPM) to solve a stationary magnetic field problem.

The program has two components: the magnetic field direct problem (used to determine the pairs of currents (i_1, i_2) for which the magnetic flux through the median yoke is null), and the field inverse problem (the reconstruction of the **B-H** relationship using the currents obtained in the direct problem).

4.1 The Magnetic Field Direct Problem—The Determination of Currents (i_1, i_2)

The magnetic circuit of the device is made of a zero-remanence ferromagnetic material. For the studied sample, one had taken into consideration two arbitrary materials with a known dependence: 1018 Steel, respectively 455 Steel. The three **B-H** dependencies are shown in Fig. 7.

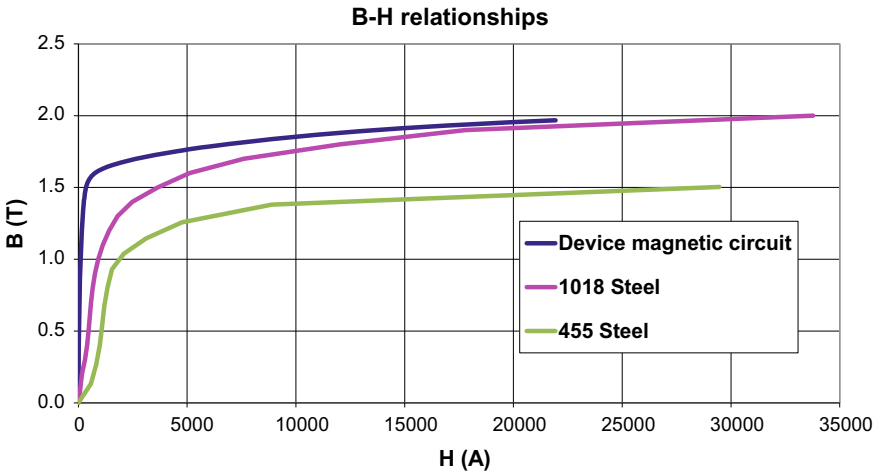

Fig. 7 B-H relationships of the device magnetic material and of the sample

Table 2 Currents (i_1, i_2) and the values of the maximum magnetic flux density for 1018 Steel sample, obtained from the direct problem

i_1 (A)	i_2 (A)	Bmax (T)
0.003	0.0989	0.1396
0.0057	0.1973	0.2751
0.009	0.296	0.4119
0.012	0.394	0.5496
0.0148	0.493	0.6872
0.018	0.593	0.82
0.0217	0.692	0.9461
0.0266	0.7915	1.0641
0.0336	0.8911	1.1754
0.0421	0.9914	1.2813
0.055	1.0916	1.3819
0.078	1.1925	1.4968
0.1144	1.294	1.6061
0.1764	1.3966	1.6645
0.2568	1.5032	1.7061
0.3712	1.6351	1.7494
0.5982	1.8948	1.8161
0.9892	2.3339	1.8934
1.752	3.0192	1.9922

Table 3 Currents (i_1, i_2) and the values of the maximum magnetic flux density of the 455 Steel sample, obtained from the direct problem

i_1 (A)	i_2 (A)	Bmax (T)
0.00860945	0.0989	0.1328
0.0128367	0.1973	0.2678
0.0163371	0.296	0.4025
0.0194525	0.394	0.5382
0.0226214	0.493	0.6736
0.0261479	0.593	0.8035
0.0302432	0.692	0.9311
0.0375819	0.7915	1.0384
0.0535341	0.8911	1.1457
0.0774609	0.9914	1.2579
0.124701	1.0916	1.38
0.284154	1.1925	1.5039
0.481376	1.294	1.62277

Tables 2 and 3 contain the pairs of currents (i_1, i_2) obtained by computing the magnetic field direct problem, respectively the samples' values of the maximum magnetic flux densities.

Figures 8 and 9 show the $i_2(i_1)$ dependencies.

Figures 10 and 11 show the magnetic flux density lines and spectre corresponding to the first pair of currents (i_1, i_2) from Tables 2 and 3. One can observe that the magnetic field is null in the median yoke.

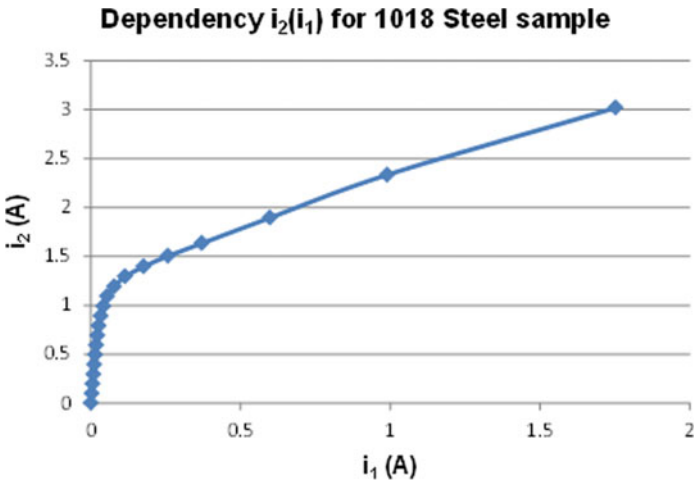

Fig. 8 Current dependency for 1018 Steel sample

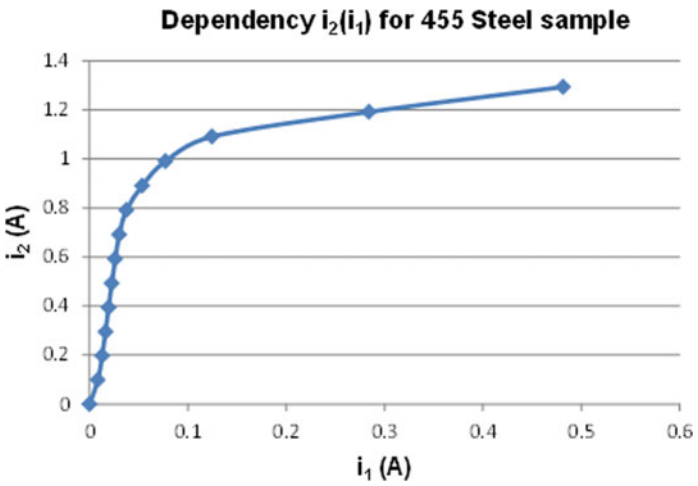

Fig. 9 Current dependency for 455 Steel sample

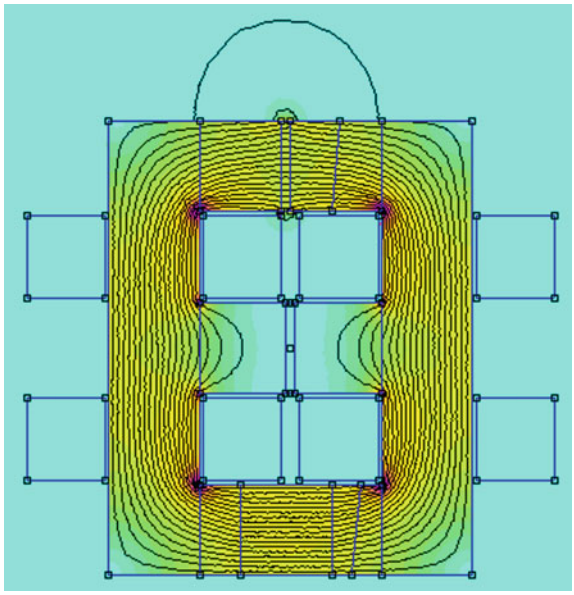

Fig. 10 Magnetic flux density lines for $(i_1, i_2) = (0.003, 0.0989)$ A—1018 Steel

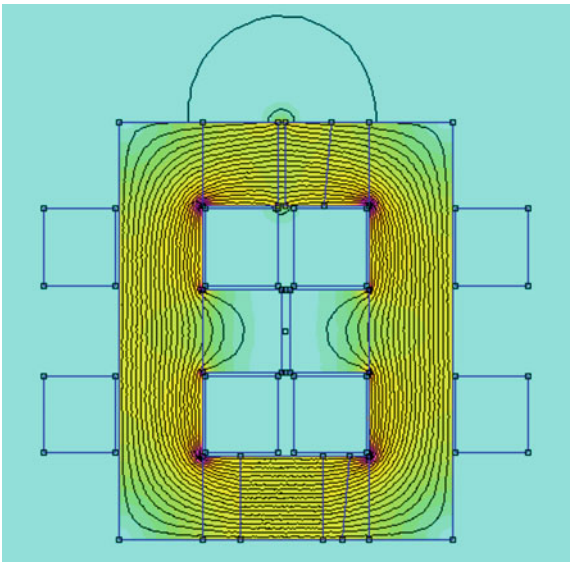

Fig. 11 Magnetic flux density lines for $(i_1, i_2) =$ (0.00860945, 0.0989) A—455 Steel

4.2 The Magnetic Field Inverse Problem—The Reconstruction of the B-H Relationship Using Currents (i_1, i_2)

Using the values of currents (i_1, i_2) from Tables 2 and 3, one reconstructs the B-H relationship of the two samples, by solving the magnetic field inverse problem. The results are shown in Figs. 12 and 13, noticing that the computed relationship is perfectly overlapped on the original one, given by the manufacturer. This proves the correctness of the proposed algorithm and device.

The device described above allows the determination of the B-H relationship by measuring the currents from two coils placed on the device columns. In the proposed procedure, one chooses a value for one of the currents. Then it searches the second one such that the value of the magnetic flux through the median yoke is zero. As a consequence, one must control the null value of the flux, a method similar to measuring resistances with the Wheatstone bridge. The values of the imposed current are ascending, also resulting in growing values for the second current. Thus, one can obtain the first magnetization curve, avoiding secondary hysteresis cycles. Then, one searches for the piecewise linear B-H relationship, by successively determining each segment of it. In the inverse problem, a segment obtained at an individual iteration describes the B-H relationship between the starting point (i.e., the maximum value of the magnetic flux density obtained in the sample for the previous pair of currents) and the ending point (i.e., the maximum magnetic flux density value obtained in the sample at the current iteration). Every magnetic flux computation presumes the

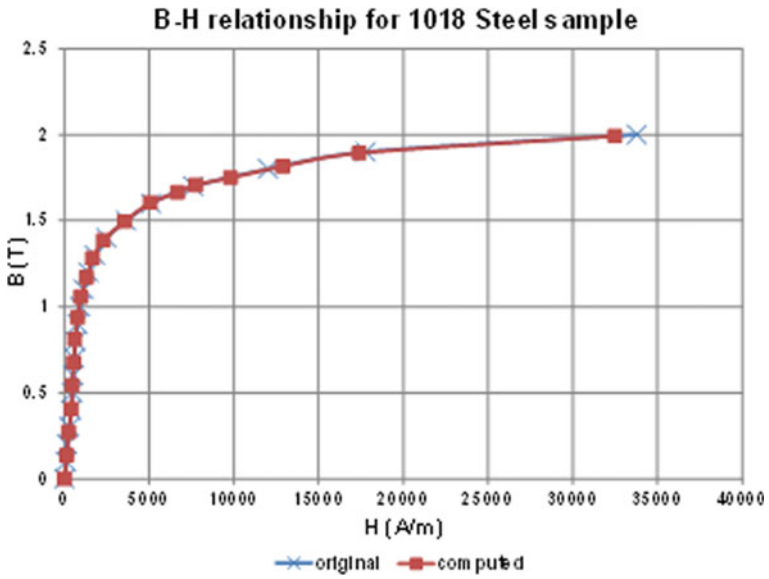

Fig. 12 Original and computed B-H relationship for 1018 Steel sample

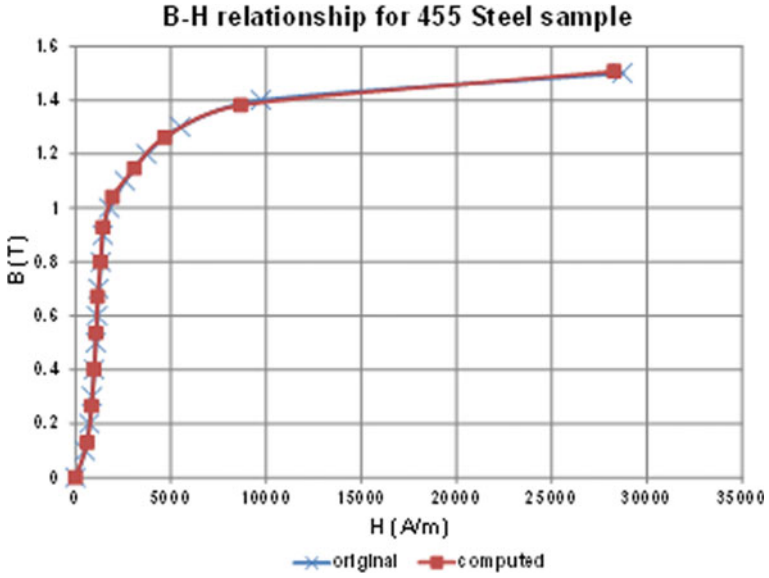

Fig. 13 Original and computed B-H relationship for 455 Steel sample

solving of a stationary magnetic field problem. The non-linearity of the B-H relationship is treated by using the iterative polarization fixed point method, and the magnetic field computation at each iteration had been made through a FEM program.

5 Conclusions

This chapter introduces the non-destructive testing field by highlighting its importance regarding safety. Non-destructive testing does not affect the integrity of the body under test, becoming therefore very important for the quality control process, subjecting the product in use or scheduled to be. The specialists in this domain have created and implemented methods and devices to characterize the materials or to detect, localize and measure the flaws (defects) with the purpose of preventing events with a high-impact such as plane crashes, nuclear power plant explosions, trains' derailment and other events which are dangerous but not very visible. The researches in NDT in the electromagnetic field look in two directions: flaw detection and flaw reconstruction. If the flaw is a crack, then the use of eddy currents testing is the most suitable procedure. For the ferromagnetic pieces, eddy currents testing has a significant disadvantage: due to the high permeability, the penetration depth is minimal, the fact which allows only surface defects detection. The best procedure of flaws detection in ferromagnetic bodies is to use the difference static magnetic field. We have a magnetic field problem in steady-state, but we must deal with the nonlinearity of the medium. Because flaw reconstruction implies a considerable computation time for the direct problem, one of the main objectives is to obtain procedures for the rapid computation of the electromagnetic field in linear/nonlinear media. Many papers in literature recommend the finite element method (FEM) or hybrid method (Finite—Boundary Element Method (FEM–BEM)).

The modification of the B-H characteristic, in aged areas, suggests the possibility of elaborating some electromagnetic detection and reconstruction procedures. The computation of the difference static magnetic field seems to be the best procedure. Because the change of the B-H characteristic is minimal, it is necessary to obtain a high accuracy computation of the magnetic field in the measurement points. This chapter falls within the field of non-destructive assessment methods by determining the B-H characteristic of ferromagnetic bodies, by using, for example, a device and a procedure for measuring the first magnetization characteristic. The main objective of this chapter is the electromagnetic field analysis, together with techniques for determining the corresponding relations. There several numerical methods available, as well as methods used to treat for the nonlinearity of the magnetization characteristics. However, only those methods able to deliver results in minimal time, with minimally allocated resources present interest. Therefore, there are presented the primary non-destructive measurement devices, in correlation with related applications. Special attention was granted to those devices used to characterize the magnetic materials widely used in energy generation, distribution and conversion, in telecommunication, aeronautics. The followed a presentation of the magnetic field analysis methods

in nonlinear media. As given an example, there is the study of the magnetization characteristic evaluation for ferromagnetic bodies. The device described in Sect. 4, allows the determination of the B-H relationship by measuring the currents from two coils placed on the device columns. The chapter ends with conclusions and many references in the non-destructive testing and electromagnetic field computation.

References

1. Stănculescu M (2009) Contribuţii la recunoaşterea formelor defectelor în defectoscopia magnetică nedistructivă (Contributions to flaw shape reconstruction in nondestructive testing). PhD thesis (in Romanian language), University "Politehnica" of Bucharest, Romania, 2008
2. SR EN ISO 9000-2001, Sisteme de management al calităţii. Principii fundamentale şi vocabular (Quality management systems. Vocabulary and fundamental principles)
3. www.asnt.org/ndt
4. IzfP Fraunhofer-Institut for NDT. https://mm.fhg.de/depts/izfp-e.html
5. Wenk SA, McMaster RC (1987) Choosing NDT: applications, costs and benefits of nondestructive testing in your quality assurance program. American Society for Nondestructive Testing, Columbus, OH
6. McMaster RC, Wenk SA (1951) A basic guide for management's choice of nondestructive tests. Special technical publication no. 112. American Society for Testing and Materials, Philadelphia, PA
7. Juran JM (1988) JURAN's quality control handbook, 4th edn. McGraw-Hill, NewYork
8. Diederichs R (2003) The advantages of the internet in the field of NDT, Internet article
9. Miller RK (1996) Nondestructive testing handbook, 2nd edn, vol 1, 2, 3, 4, 5, 6, 7, 8, 9 şi 10, American Society for Nondestructive Testing, USA
10. Cecco VS, Van Drunnen G, Sharp FL (1981) Eddy current manual: test method, vol 1, AECL-7523. Chalk River, Ontario
11. McMaster RC, McIntire P, Mester ML (eds) (1986) Non-destructive testing handbook: electromagnetic testing, vol 4, ASNT
12. de la Pintiere L (1985) Multifrequency eddy current examination of heat exchanger tubing. In: Lord W (ed) Electromagnetic methods for non-destructive testing. Gordon and Breach Science Publishers, New York, pp 195–303
13. Rao BPC, Baldev R, Jayakumar T, Kalyanasundaram P, Arnold W (2001) A new approach for restoration of Eddy current images. J Non-Destruct Eval 20:61–72
14. Ramuhalli P (2002) Electromagnetic NDE signal inversion by function-approximation neural network. IEEE Trans Magn 38(6):3633–3642
15. Takagi T, Miya K (2000) ECT Round-Robin test for steam generator tube. J Japanese Soc Appl Electromagn Mech 8:121–128
16. Chen Z, Miya K (1998) A new approach for optimal design of eddy current testing *probes*. J Nondestr Eval 17(3):105–116
17. Koch T, Browsing and searching internet resources. https://www.ub2.lu.se/nav_menu.html
18. Nondestructive evaluation *at SwRI*. https://www.nde.swri.edu/index.html
19. NTIAC. https://www.ntiac.com
20. Center for Nondestructive Evaluation at Iowa State University. https://www.cnde.iastate.edu/
21. European networks for structural integrity. https://science.jrc.nl/www/jrc/iam/sci-unit/networks/networks.html
22. DGZfP: German NDT Society. https://www.dgzfp.de
23. British Institute for NDT. https://www.powertech.co.uk/bindt/
24. The Canadian Society for Nondestructive Testing. https://www.csndt.org/
25. The NASA Technical Report Server. https://techreports.larc.nasa.gov/cgi-bin/NTRS

26. Panametrics. https://www.panametrics.com
27. Krautkramer. https://www.krautkramer.com
28. IRT—Inspection Research Technology. https://www.irt.co.il
29. Qnet. https://www.qnetworld.com
30. ASTM E 1316–1992 terminology for nondestructive examination
31. Mihai C (2003) Procedee electromagnetice nedistructive pentru evaluarea defectelor în materiale (in Romanian language), PhD thesis
32. Raj B, Jayakumar T, Rao BPC (1995) Review of NDT techniques for structural integrity. Sadhana, Acad Proc Eng Sci 20:5–38
33. Nichols RW (1982) Advances in NDE for structural integrity. Applied Science Publishers, London
34. Bllitz J (2000) Electrical and magnetic methods for non-destructive testing. Adam Hilger, Bristol
35. Lovejoy DJ (1993) Magnetic particle inspection: a practical guide. Chapman & Hall
36. Borucki JS (1991) Development of automated magnetic particle testing systems. Mater Eval 49:324–329
37. Lord W (1985) Electromagnetic methods of NDT. Gordon and Breach, New York
38. Andrei P (2015) Dispozitiv de determinare a caracteristicii de primă magnetizare pentru materiale feromagnetice (Device for determining the first magnetization curve for ferromagnetic materials). PhD thesis, PhD supervisor, Prof. PhD. Eng. I.F. Hantila, University Politehnica of Bucharest
39. Păltânea V (2008) Sisteme Avansate de Caracterizare a Materialelor Magnetice Moi (Advanced systemd for soft magnetic materials characterization). PhD thesis, PhD supervisor: Prof. PhD. Eng. H. Gavrilă, Octombrie
40. Kappel W, Caracterizarea avansată şi industrială a oţelurilor magnetice, contract 57/B Ad 1411/97/VIII, I.C.P.E
41. IEC Standard Publication 60404—2, Methods of measurement of the magnetic properties of electrical steel sheet and strip by means of the Epstein frame. IEC Central Office, Geneva, 1996
42. Sievert J, Ahlers H, Fiorillo F, Rocchino L, Hall M, Henderson L (2001) Magnetic measurements on electrical steels using Epstein and SST methods. Summary report of the EUROMET comparison project no. 489, PTB–Bericht, E−74, pp 1–28
43. Fiorillo F (2004) Measurement and characterization of magnetic materials. Elsevier Academic Press
44. Noţingher P (1995) Etude du dispositif a bande unique dans les conditions extremes de caracterisation magnetique, Stage de fin d'etudes, L.E.G.-I.N.P.G
45. Farrell E, Allen CJ, Whilden MW, Tripp JH, Usoskin A, Sheth S, Brittenham GM (2007) Magnetic measurement of liver iron stores: engineering aspects of a new scanning susceptometer based on high-temperature superconductivity. IEEE Trans Magnet 43(11):4030–4036
46. Tsukada K, Kiwa T (2007) Magnetic measurement of moisture content of grain. IEEE Trans Magnet Volo 43(6):2683–2685
47. Zijlstra H (1967) Experimental methods in magnetism, vol IX, Measurement of magnetic quantities. North–Holland publishing company, Amsterdam
48. Ochiana G, Ochiana L, Stănculescu M (2011) Teoria câmpului electromagnetic (Electromagnetic field theory), Editura Printech, 2011, ISBN 978–606–521–756–0, (214 pagini) (cod CNCSIS 54)